Korean J. Chem. Eng., **27**(5), 1428-1434 (2010)
DOI: 10.1007/s11814-010-0237-0

A study of the sulfidation and regeneration reaction cycles of Zn-Ti-based sorbents with different crystal structures

Suk Yong Jung, Jung Je Park*, Soo Jea Lee***, Hee Kwon Jun***, Soo Chool Lee*, and Jae Chang Kim*,†**

*Department of Chemical Engineering, Kyungpook National University, Daegu 702-701, Korea
**Department of Chemical Engineering, Pohang University of Science and Technology, Hyoja-dong, Nam-gu, Pohang, Gyeongbuk 790-784, Korea
***GS Fuel Cell Co., 453-2, Seongnae-dong, Gangdong-gu, Seoul 134-848, Korea
(*Received 20 October 2009 • accepted 24 December 2009*)

Abstract−The reaction cycles of the sulfidation and regeneration of Zn-Ti-based sorbents prepared by a physical mixing method (ZT-700 and ZT-1000) or co-precipitation method (ZT-cp) were tested in a fixed bed micro-reactor at middle temperature (Sulfidation; 480 °C, regeneration; 580 °C). The ZnS produced during sulfidation from the Zn_2TiO_4 with a spinel structure (ZT-1000, ZT-cp) was easily regenerated even at 550 °C, while the ZnS produced from the ZnO with a hexagonal structure (ZT-700) needed a temperature higher than 610 °C. After regeneration, each sorbent was restored to its original crystal structure. The differences in the regeneration properties and the reaction cycles of the sorbents were related to the original crystal structures rather than to the physical properties such as pore volume and surface area. To study these differences further, FT-IR, FT-Raman, XRD and TPR were used, and their results including the reaction cycles of the sulfidation and regeneration on the Zn-Ti based sorbents with different crystal structures were discussed.

Key words: Desulfurization, Regeneration, Sorbent, Hot Coal Gas, Crystal Structure, Reaction Cycles

INTRODUCTION

Coal is extremely abundant and more widely distributed in comparison with other fossil fuels like natural gas and oil. In addition, coal is one of the most abundant fossil fuel sources on earth with reserves available for several hundred years. For these reasons, coal is expected to maintain a significant share of this demand for the near future. So far, coal has been mostly used for electricity generation, which has produced various pollutants such as SOx and NOx. Recently, for the environmental and efficient use of coal, several thermal cycles with coal as fuel have been proposed, such as the pressurized fluidized bed combustion (PFBC) and integrated gasification combined cycle (IGCC) [1]. In particular, IGCC is considered to be among the most efficient and environmentally acceptable technologies for the generation of power from coal. IGCC systems are capable of significantly lower discharge rates of gaseous, liquid, and solid wastes relative to conventional coal-based systems [2]. IGCC technology is an environmentally benign power generation technology advanced by many developed countries with funding of several billions of dollars until now. The most critical cost and the risks involved with a construction cost for the plant. But the construction cost of a coal IGCC plant after 2010 is expected to drop to less than US$ 1100 kW. With higher efficiency and less generation of pollutants, it would be cheaper than the pulverized coal power plants installed with desulfurization and de-NOx facilities [3]. To use this technology, it is necessary to remove the pollutants from the coal-derived fuel gas. Among the pollutant gases, sulfur, which exists in the form of H_2S or COS under the highly reducing condition of a gasifier, must be removed from the hot coal gas because these species entering the gas turbine are converted to SOx, which are known as precursors of acid rain and whose emission into the atmosphere is limited by strict government regulation. In addition, the H_2S gases cause corrosion of the turbine and deactivation of the catalyst used in other processes such as NH_3 decomposition process, water gas shift reaction and CO_2 absorption process et al. [1-4].

Typically, several commercial techniques are available for the removal of H_2S and COS using a Selexol and similar processes [2]. However, the disadvantage of these commercial techniques for the purification of coal gas is that the hot coal gas must be cooled to an ambient temperature and then preheated to a high temperature before it can be used in a gas turbine. To avoid heat loss and save energy, high (higher than 550 °C) or middle (350-550 °C) temperature desulfurization technology has been widely developed and appears to be the major technique for the removal of hydrogen sulfide from hot coal gas [2,3]. An IGCC system with hot-gas clean up is a process that shows promise for higher thermal efficiency and superior environmental performance than the conventional process. Although thermal efficiencies of 30-35% are typical for conventional pulverized coal plants, efficiencies of 43-46% may be easily attainable by IGCC with hot gas cleanup [5].

Recent studies have indicated that desulfurization system components become prohibitively expensive with increasing operating temperature and that the overall IGCC process efficiency gains of carrying out desulfurization above 550 °C may not be sufficient to justify operation at such high temperature. Due to equipment limitations and other variables, the optimum temperature for fuel gas desulfurization in this process is estimated to be between 350 and 550 °C (middle temperature range), where technical viability and process efficiency result in a lower overall process cost [6].

†To whom correspondence should be addressed.
E-mail: kjchang@knu.ac.kr

Several metal oxides, such as Ca-based sorbent [7], Zn-based sorbent [8-10], Cu-based sorbent [11-13], Mn-Fe-Zn containing sorbent [14,15] et al., have been studied for the development of regenerable sorbents to remove hydrogen sulfide from coal-derived gas in high or middle temperature ranges under severe reduction conditions.

The affinity of many metal oxides for reduced sulfur species is improved as the temperature is decreased, making many solids potentially suitable for hot gas clean up applications in the middle temperature range. Especially, the Zn-Ti based sorbents are known to be among the best metal oxide sorbents, having the most favorable thermodynamics for H_2S removal and regeneration properties in the middle temperature range. In this temperature range, the conventional Zn-Ti based sorbents prepared by the physical mixing method have shown some inferior properties such as low initial sulfur capacity, regeneration properties and deactivation with an increase in cycle number [16-19]. To solve these problems, various promoters, such as cobalt [20-23], nickel [21-23] and iron [24] et al., were added to the Zn-Ti based sorbents. The sorbents with an excellent sulfur removing capacity could be prepared throughout the co-precipitation of these promoters. Jung et al. [17] also reported that the sulfur-removing capacity of the Zn-Ti based sorbent depended on the physical properties, such as pore volume, pore size and surface area et al. But, the details of the study on the different crystal structures formed by various preparation methods and pretreatment conditions, which are expected to severely affect their sulfidation and regeneration behaviors, have not yet been understood.

In this work, to investigate these behaviors and the sulfidation/regeneration cycles with different crystal structures, Zn-Ti based sorbents were prepared by various methods such as the co-precipitation and physical mixing method and tested in a fixed-bed reactor at a middle temperature range. In addition, the changes of crystal structure and physical properties of the sorbents before and after the reaction were compared with the aid of Hg porosimetry, X-ray diffraction (XRD: Philips, X'PERT) and Fourier transform infrared (FT-IR: Mattson Instruments Inc., Galaxy 7020A).

EXPERIMENTAL

1. Preparation of the Sorbent

1-1. Physical Mixing Method

The ZT-700 and ZT-1000 sorbents used in this study were prepared by the physical mixing method. Zinc oxide and titanium dioxide, with a particle size of about 250-300 mesh, were mixed with an inorganic binder, bentonite, for 1-2 hrs. Next, a liquid binder, ethylene glycol (EG), was added to the mixture to make the slurry. An extruder was used to form pellets from the slurry with an outer diameter of 1 mm. These wet pellets were dried at a temperature of 150 °C for 4 hrs to remove ethylene glycol from the material. The dried pellets were calcined in a muffle furnace for 4 hrs at 700 °C (ZT-700) and 1,000 °C (ZT-1000), and then ground to a particle size ranging between 250-300 μm in diameter. The ramping rate of the temperature was maintained at 3 °C/min. The mole ratio of Zn to Ti was fixed at 1.5 : 1.

1-2. Co-precipitation Method

The ZT-cp sorbents used in this study were prepared by co-precipitation. Metal salts such as Zinc nitrate and Titanium sulfate, were dissolved in water. Precipitation was carried out by adding a raw salt solution to the NaOH (1.5 mol solution) under vigorous mixing at room temperature. The product of the precipitation was aged for 12 hrs, and then washed and separated by filtration. An extruder was used to form pellets from the slurry with an outer diameter of 1 mm. The product was dried at 150 °C, calcined at 700 °C, and then ground to a particle size ranging between 250-300 μm in diameter. In addition, in order to identify crystalline phases in the mixed oxides, an X-ray diffraction (XRD) study was performed with a Philips XPERT instrument using a CuKα radiation source at the Korea Basic Science Institute.

2. Apparatus and Procedure

Multiple cycles of sulfidation/regeneration were performed in a fixed-bed quartz reactor with a diameter of 1 cm in an electric furnace. One gram of sorbent was packed into the reactor and the space velocity (SV) was maintained at 5,000 h^{-1} to minimize a severe pressure drop and channeling phenomena. All of the volumetric gas flows were measured under standard temperature and pressure (STP) conditions. The temperature of the inlet and outlet lines of the reactor was maintained above 120 °C to prevent the condensation of water vapor in the sulfidation process. The outlet gases from the reactor were automatically analyzed every 8 min by a thermal conductivity detector (TCD) equipped with an auto-sampler (Valco). The column used in the analysis was a 1/8-in. A teflon tube was packed with Porapak T. The sulfidation and regeneration conditions and the composition of mixed gases are shown in Table 1. When the H_2S concentration of the outlet gases reached 15,000 ppmv, the concentration of H_2S at the inlet stream of mixed gases, an inert nitrogen gas without H_2S, was introduced to purge the system until it reached the regeneration temperature. Finally, nitrogen gas mixed with 3% oxygen was introduced to regenerate the sulfurized sorbents until the SO_2 concentration reached 200 ppm.

RESULTS AND DISCUSSION

1. The Regeneration Property

The regeneration characteristics are among the most important factors to be considered, as well as the sulfur removing capacity. Fig. 1(a) shows the SO_2 breakthrough curves of the ZT-1000, ZT-700 and ZT-cp sorbents during regeneration after the first sulfidation process at the middle temperature range. Nitrogen gas mixed with 3% oxygen was introduced to regenerate the sulfided sorbents until the SO_2 concentration reached a value less than 200 ppmv. From the stoichiometric coefficient of the regeneration reaction equation

Table 1. Experimental conditions

	Sulfidation process		Regeneration process	
Temperature (°C)	480 °C		580 °C	
Pressure (atm)	1		1	
Flow rate (mL/min)	50		50	
Gas composition (%)	H_2	11.7	O_2	3
	CO	9.552	N_2	Balance
	CO_2	5.2		
	H_2S	1.5		
	N_2	Balance		

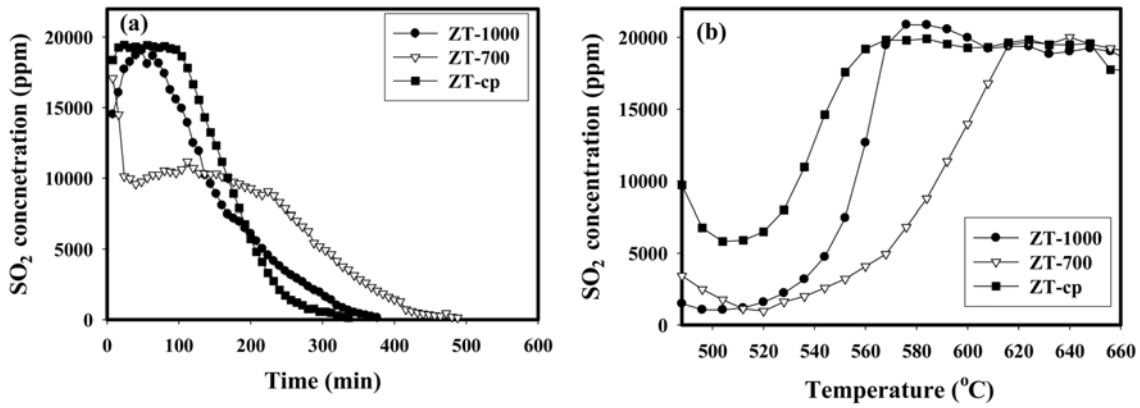

Fig. 1. The SO_2 breakthrough curves (a) and TPR (temperature programmed regeneration) results (b) of the ZT-1000, ZT-700 and ZT-cp sorbents at 580 °C.

for the Zn-based sorbents ($ZnS+3O_2 \rightarrow ZnO+2SO_2$), 2 mol of SO_2 were produced when 3 mol of oxygen were consumed during regeneration. In the case of the ZT-1000 and ZT-cp sorbents, the maximum SO_2 concentration was maintained until 60 min and 120 min, respectively, and both the concentrations rapidly decreased. In the case of the ZT-700 sorbent, a level of 10,000 ppmv of the SO_2 concentration was maintained during the initial regeneration process, and then the concentration gradually decreased. 1.46 times the regeneration time was needed for the ZT-700 sorbent compared to that for the ZT-cp sorbent. In Fig. 1(b), the results of the TPR (temperature programmed regeneration) tests are shown. The tests were carried out by measuring the concentration of SO_2 desorbed from the sorbents sulfided, when the ramping rate of the temperature was 1 °C/min and mixed nitrogen gas containing 3% oxygen was used. In the case of the ZT-1000 and ZT-cp sorbents, the maximum SO_2 concentration was found at 550 °C and 570 °C, respectively. In the

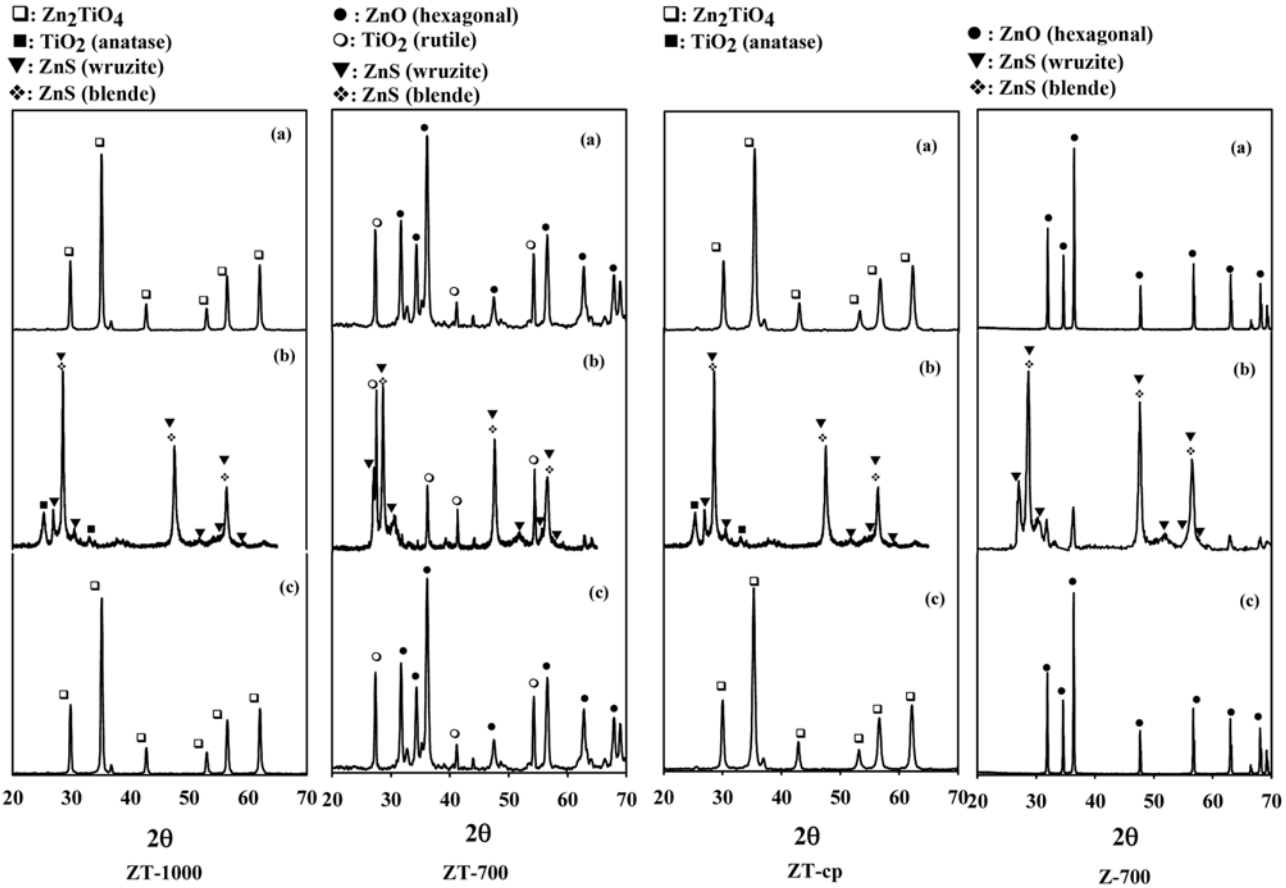

Fig. 2. The XRD patterns of the ZT-1000, ZT-700, ZT-cp and Z-700 sorbents (a) on the fresh, (b) after sulfidation process and (c) after regeneration process.

case of the ZT-700 sorbent, most of the sulfur was desorbed above 600 °C [17].

2. The Crystal Structures of the Sorbents

To explain the different regeneration properties, the crystal structures of the ZT-1000, ZT-cp and ZT-700 sorbents before/after reaction were characterized by using XRD, FT-IR and FT-Raman. The XRD pattern after sulfidation and regeneration of each sorbent is shown in Fig. 2. The crystal structures of the ZT-1000 and ZT-cp sorbents, before H_2S absorption, were assigned to Zn_2TiO_4, a general spinel structure without an unreacted single oxide such as zinc oxide or titanium dioxide. The ZT-700 sorbent, however, consisted of a separate zinc oxide hexagon structure and titanium oxides having a rutile structure without a spinel structure owing to the low pretreatment temperature. The origin of the spinel structure of the ZT-cp sorbent was believed to be due to the relatively small nanoparticle size formed even at the low pretreatment temperature (700 °C). After the sulfidation process, in the case of the ZT-1000 and ZT-cp sorbents, both structures were changed to zinc sulfides and titanium dioxides. The main 2θ angles of the zinc sulfide were found at 28, 47.5 and 56.4, which were defined as a zinc blende with a cubic structure. Most of the structures after the sulfidation process existed as this zinc blende structure. In addition, small amounts of zinc wrutzite having a hexagonal structure were found at 2θ angles of 26.99, 28.5, 30.17, 47.5 and 56.4. In the case of titanium dioxide, its main 2θ angles were found at 2θ angles of 25 and 31, which were defined as the anatase structure of an orthorhombic structure. In the case of the ZT-700 sorbent, the similar main 2θ angles of the zinc sulfide were found at 26.7, 28.5, 30.17, 47.5 and 56.4. However, the intensity of the zinc wrutzite structure was more intense than that of the zinc blende structure. It could be estimated by the peak height that the amount of the zinc wrutzite was very similar to the amount of the zinc blende. The 2θ angles of the titanium dioxide were shown at 27, 32 and 42, which were defined as the rutile structure of a tetragonal structure.

From the above results, it could be found that two kinds of zinc sulfide forms (blende and wrutzite) existed after sulfidation. In the case of the zinc sulfides produced from the spinel structure (ZT-1000 and ZT-cp), most of them existed as zinc blende structures, while in the case of the zinc sulfides produced from the single zinc oxide of the hexagonal structure (ZT-700), a similar amount of zinc blende and wrutzite structures coexisted. To compare the differences in the crystal structure between the spinel structure and single zinc oxide under the same reaction conditions, the Z-700 sorbent was prepared by using only the zinc oxide without titanium. Physical mixing was used and they were calcined at 700 °C. Its XRD patterns had the same characteristics as the zinc oxide of the ZT-700 sorbent. These results also agreed with those reported by Sasaoka et al. [25].

After regeneration, in the case of the ZT-1000 and ZT-cp sorbents, their sulfide forms were returned to Zn_2TiO_4 with a spinel structure, but without the zinc oxide of the hexagonal structure or the titanium dioxide of the rutile structure. In the case of the ZT-700 sorbent, its sulfide form was returned to the zinc oxide with a hexagonal structure and TiO_2 with a rutile structure. In the case of the Z-700 sorbent, its sulfide form was returned to zinc oxide in a hexagonal structure. To confirm the structural differences of the zinc sulfides after the sulfidation process, the sulfide forms of all the sorbents were characterized using FT-IR and Raman spectroscopy. Fig. 3(a) shows the FT-IR results of the ZT-based sorbents after sulfidation. In the case of the ZT-cp and ZT-1000 sorbents, their absorption wavenumber was about 323.7 cm^{-1}, which was found for most zinc sulfides of cubic form through XRD results. However, in the case of the ZT-700 and Z-700 sorbents, the absorption wavenumber was about 304.7 cm^{-1}, which had shifted to the left by as much as 20 cm^{-1}. This meant that the sulfide forms of the ZT-700 and Z-700 sorbents were in different patterns from those of the ZT-1000 and ZT-cp sorbents. From the XRD results, it was found that the wrutzite structures of the ZT-700 and Z-700 sorbents were much more prevalent than those of the ZT-cp and ZT-1000 sorbents. Fig. 3(b) shows the FT-Raman spectroscopy of the ZT-based sorbents after sulfidation. In the case of the ZT-cp and ZT-1000 sorbents, the wavenumbers of 143, 396, 515 and 638 cm^{-1} could be assigned as titanium oxide with an anatase structure. In the case of the ZT-700 and Z-700 sorbents, the wavenumbers of 226, 448 and 610 cm^{-1} could be assigned as titanium oxide with a rutile structure. These results were identified with the XRD patterns of titanium oxide after sulfidation of the sorbents reported in a previous paper [26].

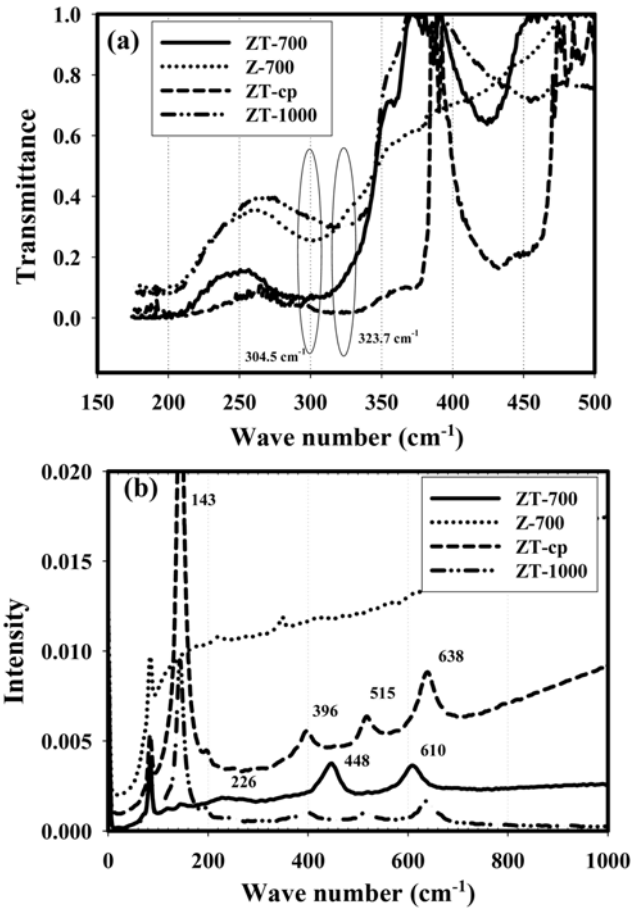

Fig. 3. The FT-IR (a) and the FT-Raman (b) results of the Z-700, ZT-700, ZT-1000 and ZT-cp sorbents after sulfidation process.

3. The Physical Properties of the Sorbents

To investigate the influence of the physical properties on the regeneration properties of the sorbents, the physical properties such

Table 2. The physical properties of various Zn-Ti-based sorbents before and after sulfidation process

Sorbents		Surface area (m^2/g)	Pore cumulative volume (mL/g)	Main pore size (nm)
ZT-1000	Fresh	3.24	0.31	378.9
	Sulfidation	2.36	0.14	254.1
ZT-700	Fresh	8.43	0.29	124.3
	Sulfidation	5.86	0.26	133.7
ZT-cp	Fresh	18.34	0.89	210.4
	Sulfidation	16.04	0.40	204.9

as surface area, pore volume and particle size of the sorbents before and after sulfidation were measured by the porosimetry and BET. Table 2 shows the surface area of the ZT-1000, ZT-cp and ZT-700 sorbents before and after sulfidation. The surface area of the ZT-1000 and ZT-700 sorbents after sulfidation was 2.36 and 5.86 m^2/g, respectively. In the case of the ZT-cp sorbents, its surface area was 16.04 m^2/g, which was a larger value than those of the ZT-1000 and ZT-700 sorbents. Fig. 4 shows incremental pore volumes of the various sorbents before (a) and after (b), the sulfidation process. As shown in Fig. 4, the main pore sizes of the ZT-1000, ZT-700 and ZT-cp sorbents before and after the sulfidation process were not changed, but their pore volumes were decreased after the sulfidation process. As shown in Table 2 and Fig. 4, it was found that the cumulative pore volume and surface area of the sorbents before the sulfidation process were larger than those of the sorbents after the sulfidation process. These results were due to the expansion of the sorbents when the metal oxide was transformed to a metal sulfide. In addition, the results showed that the physical properties such as pore volume and surface area of the ZT-700 sorbent were larger than those of the ZT-1000 sorbent after sulfidation process, but lower than those of the ZT-cp sorbent. In comparison with the regeneration properties of the ZT-700 and ZT-cp sorbents, the regeneration ability of the ZT-700 sorbent was markedly low. Even though the physical properties of the ZT-1000 sorbent were lower than those of the ZT-700 sorbent, the regeneration property of the ZT-1000 sorbent was higher than that of the ZT-700 sorbent. Considering the orders of these physical sizes, the general effects of the physical properties on the regeneration properties were not found.

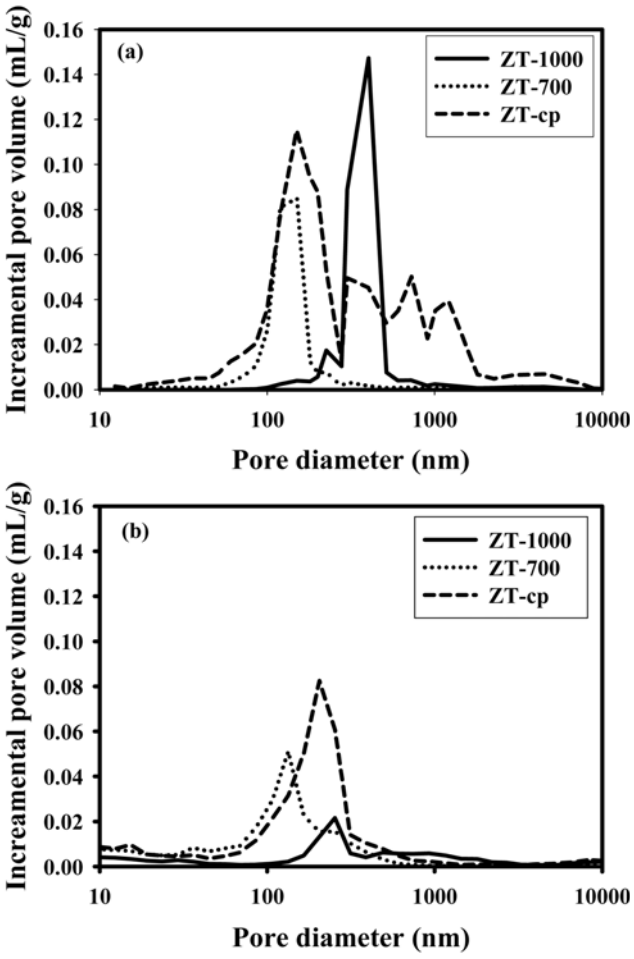

Fig. 4. The pore distribution of the ZT-1000, ZT-700 and ZT-cp sorbents before (a) and after (b) sulfidation process.

4. A Study of the Sulfidation and Regeneration Cycles with Different Crystal Structures

A previous research study reported that the sulfur-removing capacity of the sorbent was related to the physical properties such as surface area, pore volume and particle size rather than crystal structure [17]. In particular, the sulfur-removing capacity of the ZT-cp sorbent with the large pore volume, surface area and nano particle size was better than that of the other sorbents (ZT-700, ZT-1000). However, in the case of regeneration properties, ZT-cp sorbent and ZT-1000 sorbent showed a very similar tendency which was independent of their physical properties. Although the ZT-700 sorbent had a larger surface and pore volume than the ZT-1000 sorbent, the regeneration property of the ZT-1000 sorbent was better than that of the ZT-700 sorbent. Considering the different regeneration properties and their different crystal structures, the reaction cycles with different crystal structures of the sorbents could be proposed. Fig. 5(a) shows a plausible proposal for the reaction cycles of the ZT-cp and ZT-1000 sorbents. The structure of zinc sulfide converted from Zn_2TiO_4 of spinel structure during sulfidation was mostly zinc blende in the cubic crystal system with some amount of zinc wrutzite. In the cubic crystal system, zinc and sulfur atoms are tetrahedrally coordinated. The structure is closely related to the structure of a diamond. It forms ABCABC layers. The zinc wrutzite structure is a member of the hexagonal crystal system and consists of tetrahedrally coordinated zinc and sulfur atoms that are stacked in an ABABAB pattern [27]. In addition, the titanium oxide converted from Zn_2TiO_4 during sulfidation had an anatase structure. The spinel structure has the form of AB_2O_4, where A is a metal ion with a +2 valence and B is a metal ion with a +3 valence. This structure is viewed as a combination of the rock salt and zinc-blend structures as shown in Fig. 5(a). The oxygen ions are in face-centered cubic close packing. A and B ions occupy tetrahedral and octahedral interstitial sites. The spinel structure can be divided into two types: normal and inverse spinel. In normal spinels, A^{2+} ions are on tetrahedral sites and the B^{3+} ions are on octahedral sites. In inverse spinels, the A^{2+} ions and half of the B^{3+} ions are on octahedral sites; the other half of the B^{3+} are on tetrahedral sites, $B(AB)O_4$. The Zn_2TiO_4 structure corresponded to an inverse spinel structure [28,29]. The half of the zinc oxide in an inverse spinel structure was formed on the tetrahedral site and

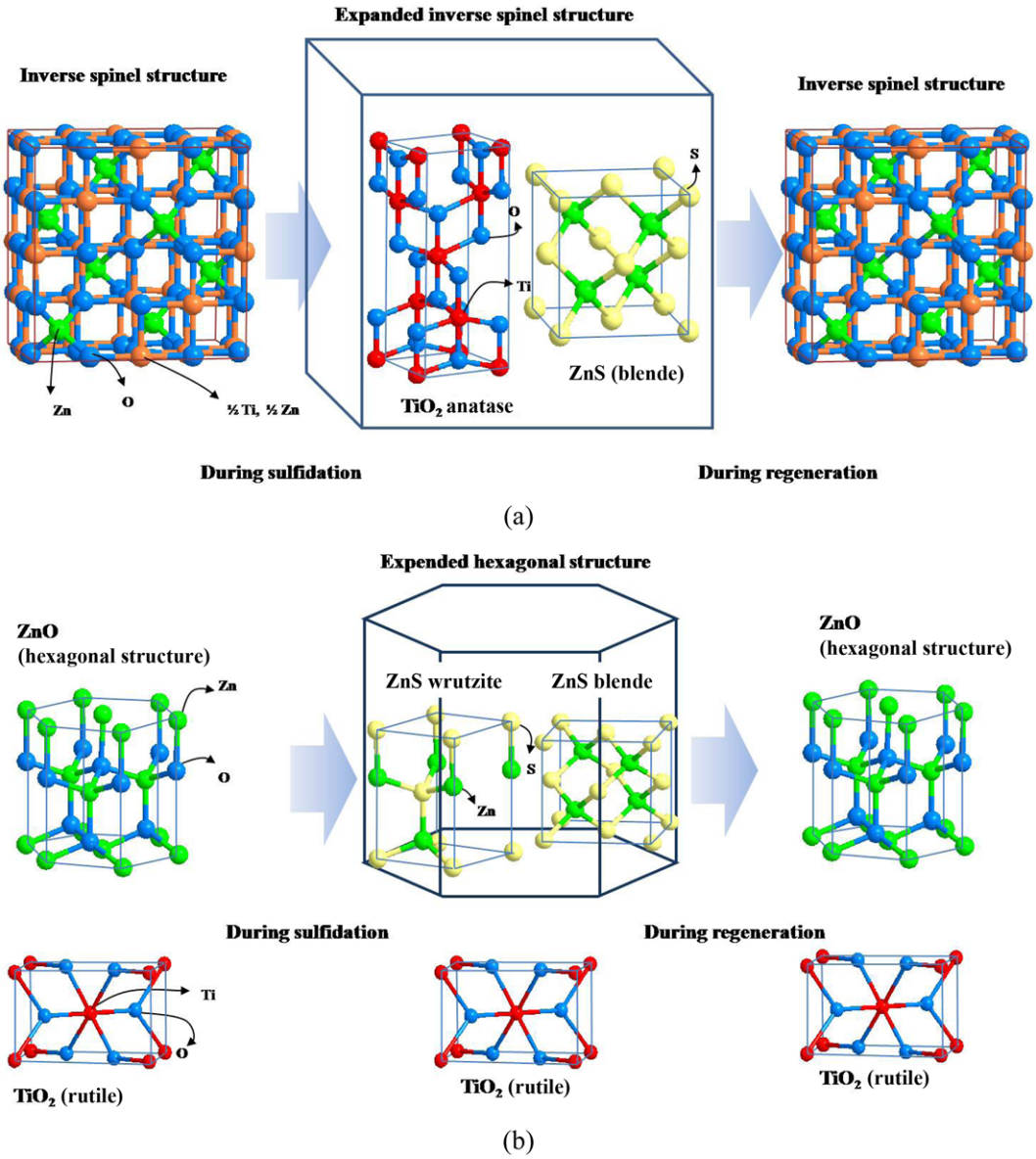

Fig. 5. (a) The reaction mechanism (I) proposed for ZT-1000 and ZT-cp sorbents and (b) the reaction mechanism (II) proposed for the Z-700 and ZT-700 sorbents.

the other half on the octahedral site. The titanium oxide was formed as a rock salt on the octahedral site in an inverse spinel structure. Consequently, when the zinc oxides on the inverse spinel structure were converted to zinc sulfides, which were almost all of a zinc blende form and a little of a zinc wrutzite form, the zinc titanate of the spinel structure (Zn_2TiO_4) was not broken into separated zinc sulfide and titanium oxide. In previous results, during the sulfidation process, the titanium oxide did not remain in an octahedral form but changed to an orthorhombic form such as an anatase structure confirmed by Raman and XRD after sulfidation. It was believed that the titanium oxides in an octahedral form in a unit cell of the inverse spinel structure were distorted to the titanium oxide in an orthorhombic structure (anatase) by the expanded zinc sulfides because the volume of sulfur (15 cm^3/mol) was larger than that of oxygen (14 cm^3/mol). And then, during the regeneration process, the zinc sulfides were returned to zinc oxides and the titanium oxides in an orthorhombic structure were also returned to an octahedral form in a unit cell of the inverse spinel structure. At the same time the original crystal structure, zinc titanate (Zn_2TiO_4), was restored. If the zinc titanate were broken down to the separate zinc sulfide and titanium oxide during the sulfidation process, the separate zinc sulfide and titanium oxide could not be restored to the alloyed form of the zinc titanate (Zn_2TiO_4) because the synthesis of the zinc titanate (Zn_2TiO_4) from the separate zinc oxide and titanium oxide needs a very high temperature above 1,000 °C [28-31]. Therefore, in the middle temperature range, it was believed that the inverse spinel structure like the zinc titanate (Zn_2TiO_4) was not broken down into a separated zinc sulfide and titanium oxide during sulfidation process but was distorted by the expansion when the zinc oxide was converted to zinc sulfide in a unit cell of the inverse spinel structure [32]. So, during the regeneration process, the zinc sulfide and titanium oxide could be easily restored to the original zinc titanate (Zn_2TiO_4) of the spinel

structure even at 550 °C.

Fig. 5(b) shows the possible reaction cycles for the ZT-700 and Z-700 sorbents. In the case of the ZT-700 and Z-700 sorbents, the zinc oxide had only a hexagonal structure and it was changed to zinc sulfide during the sulfidation process. From XRD results, two kinds of zinc sulfide crystal forms, the zinc blende structure and the zinc wrutzite structure, were found. As compared with XRD results of the ZT-1000 and ZT-cp sorbents, the specific peak intensity of the zinc wrutzite structure of the ZT-700 and Z-700 sorbents was higher than that of the ZT-cp and ZT-1000 sorbents. In addition, from the FT-IR results, it was confirmed that the specific wave number (304.7 cm^{-1}) of the zinc sulfides converted from the zinc oxides of hexagonal structure was different from that (323.7 cm^{-1}) of the zinc sulfides converted from the zinc titanate (Zn_2TiO_4) in the inverse spinel structure. It was believed that the wrutzite structure was converted from the zinc oxide-like hexagonal structure and the blende structure was produced by the expansion phenomenon when the zinc sulfide-like wrutzite structure with some amount of blende structure was formed from zinc oxide in a hexagonal structure. To convert the zinc sulfides back again to the original zinc oxide with a hexagonal structure, it is necessary to have a regeneration temperature above 610 °C which could be proved through the previous TPR result.

CONCLUSION

The Zn-Ti based desulfurization sorbents showed different sulfidation/regeneration reaction cycles depending on the initial states of crystal structures formed during preparation. In the case of the zinc titanate (Zn_2TiO_4) with spinel structure prepared by incipient method, the Zn_2TiO_4 was converted to the zinc sulfide with mainly blende structure and a little wrutzite structure and titanium oxide with orthorhombic structure (anatase) during sulfidation process without breaking into a separate phase, and then, the zinc sulfide and titanium oxide distorted by the expansion could be easily restored to their original spinel structure even at a temperature lower than 550 °C. Whereas, the zinc oxides with hexagonal structure prepared by the physical mixing method, were converted to the zinc sulfide with wrutzite and blende structure which was distorted by the expansion of the sorbents, and then, the zinc sulfides were restored to their original zinc oxides with a hexagonal structure at a temperature higher than 610 °C.

ACKNOWLEDGEMENT

This work was supported by the Korea Science and Engineering Foundation (KOSEF) grant funded by the Korea government (MEST) (No. 20090081082).

REFERENCES

1. H. C. Frey and E. S. Rubin, *Environ. Sci. Technol.*, **26**(10), 1982 (1992).
2. C. O. Bauer, *Environ. Sci. Technol.*, **37**(1), 27A (2003).
3. Y. S. Yun, Y. D. Yoo and S. W. Chung, *Fuel Process. Technol.*, **88**, 107 (2007).
4. L. Zheng and E. Furinsky, *Energy Conver. Manage.*, **46**, 1767 (2005).
5. L. D. Gasper-Galvin, A. T. Atimtay and R. P. Gupta, *Ind. Eng. Chem. Res*., **37**, 4157 (1998).
6. R. B. Slimane and J. Abbasian, *Advances in Environ. Res.*, **4**, 147 (2000).
7. A. Abad, J. Adanez, F. Garcial-Labiano, L. F. de Diego and P. Gayun, *Energy & Fuel*, **18**(5), 1543 (2004).
8. S. Lew, K. Jothimurugesan and M. Flytzani-Stephanopoulos, *Ind. Eng. Chem. Res*., **28**, 535 (1989).
9. T. H. Ko, H. Chu, H. P. Lin and C. Y. Peng, *J. Hazard. Mater.*, **136**, 776 (2006).
10. J. M. Sanchez-Hds4ervas, J. Otero and E. Ruiz, *Chem. Eng. Sci.*, **60**, 2977 (2005).
11. T. Kyotani and H. Kawashima, *Environ. Sci. Technol.*, **23**(2), 218 (1989).
12 E. Garcia, J. M. Palacios, L. Alonso and R. Moliner, *Energy & Fuels*, **14**, 1296 (2000).
13. J. Abbasian and R. B. Slimane, *Ind. Eng. Chem. Res*., **37**, 2775 (1998).
14. J. C. Zhang, Y. H. Wang and R. Y. Ma, *Fuel Process. Technol.*, **84**, 217 (2003).
15. J. C. Zhang, Y. H. Wang and D. Y. Wu, *Energy Conver. Manage.*, **44**(3), 357 (2003).
16. L. Alonso, J. M. Palacios and R. Moliner, *Energy & Fuels*, **15**, 1396 (2001).
17. S. Y. Jung, H. K. Jun, S. J. Lee, T. J. Lee, C. K. Ryu and J. C. Kim, *Environ. Sci. Technol.*, **39**(23), 9324 (2005).
18. S. O. Ryu, N. K. Park, C. H. Chang, J. C. Kim and T. J. Lee, *Ind. Eng. Chem. Res*., **43**(6), 1466 (2004).
19. K. Jothimurugesan and S. K. Gangwal, *Energy & Fuel*, **37**(5), 1929 (1998).
20. H. K. Jun, T. J. Lee, S. O. Ryu and J. C. Kim, *Ind. Eng. Chem. Res*., **40**, 3547 (2001).
21. H. K. Jun, T. J. Lee, S. O. Ryu, C. K. Yi, C. K. Ryu and J. C. Kim, *Energy & Fuel*, **18**(1), 41 (2004).
22. H. K. Jun, S. Y. Jung, T. J. Lee and J. C. Kim, *Korean J. Chem. Eng*., **21**(2), 425 (2004).
23. H. K. Jun, S. Y. Jung, T. J. Lee, C. K. Ryu and J. C. Kim, *Catal. Today*, **87**, 3 (2003).
24. H. K. Jun, T. J. Lee and J. C. Kim, *Ind. Eng. Chem. Res*., **41**, 4733 (2002).
25. M. Hatori, E. Sasaoka and Md. A. Uddin, *Ind. Eng. Chem. Res*., **40**, 1884 (2001).
26. J. V. Ibarra, C. Cilleruelo, E. Garacia, M. Pineda and J. M. Palacios, *Vibrational Spectroscopy*, **16**, 1 (1998).
27. J. Hauck and K. Mika, *J. Solid State Chem.*, **138**, 334 (1998).
28. S. K. Manik and S. K. Pradhan, *Physica*, **E 33**, 69 (2006).
29. C. F. Li, Y. Bando, M. Nakamura, N. Kimizuka and H. Kito, *Mater. Res. Bull.*, **35**, 351 (2000).
30. Z. W. Wang, S. K. Saxena and C. S. Zha, *Physical Review*, **B 66**, 024103-1 (2002).
31. Y. Yang, X. W. Sun, B. K. Tay, J. X. Wang, Z. L. Dong and H. M. Fan, *Advanced Materials*, **19**, 1839 (2007).
32. S. C. Kang, H. K. Jun, T. J. Lee, S. O. Ryu and J. C. Kim, *Korean Chem. Eng. Res.*, **40**, 289 (2002).